https://doi.org/10.1016/j.jobe.2020.101932

Development of vulnerability curves of buildings to windstorms using insurance data: An empirical study in South Korea

Sang-Guk Yum [1], Ji-Myong Kim [2] and Hsi-Hsien Wei [3,*]

[1] Department of Civil Engineering and Engineering Mechanics, Columbia University, New York, NY 10027, USA; sy2509@columbia.edu

[2] Department of Architectural Engineering, Mokpo National University, Mokpo 58554, Korea; jimy6180@gmail.com

[3] Department of Building and Real Estate, The Hong Kong Polytechnic University, Kwoloon, Hong Kong, PR China; hhwei@polyu.edu.hk, hhweing@gmail.com

* Correspondence: hhwei@polyu.edu.hk, hhweing@gmail.com; Tel.: +852-3400-8194

Abstract: Windstorms cause a range of damage to the built environment. Although numerous risk-assessment models for estimating such damage have been developed, the results generated by these models are often inaccurate due to the incompleteness and/or poor quality of the regional-scale building information that they require. As an alternative, therefore, this study utilizes an insurance company's loss data pertaining to the high winds of Typhoon Maemi in South Korea in 2003 to calculate building damage in terms of damage ratios. Next, these damage ratios and storm-wind speeds are utilized to construct vulnerability curves that can be used to predict levels of damage to designated building types that are subjected to given wind speeds. Lastly, geographical information systems spatial data is combined with those vulnerability curves to arrive at four distinct wind-damage states. It is hoped that the present research will serve as a reference for further development of building vulnerability curves for storm winds.

Keywords: Natural disasters; risk management; vulnerability curves; wind storm

1. Introduction

Over the past two decades, the severity of major storms and the damage they cause has rapidly increased. For example, Hurricane Katrina in 2005 devastated and paralyzed the Gulf Coast, causing US$108 billion worth of damage, making it the costliest natural disaster in U.S. history [1]. Hurricanes Ike in 2008 and Sandy in 2012 caused about US$29.5 billion and US$71.4 billion in damage, respectively. In 2013, Super-typhoon Yolanda – also known as Typhoon Haiyan – caused similar levels of damage in Southeast Asia, which were valued at nearly US$2.9 billion [2].

Investigating damage caused by high winds of various speeds is crucial to public-policy makers' risk-mitigation plans, as well as to insurance-industry decision-making about insurance premiums. Accordingly, governments, the insurance industry, and also the construction industry have developed a variety of risk-assessment models for estimating the damage to buildings caused by strong winds at the regional and national levels. In the specific case of windstorms, such models can be used to estimate the values of probable property loss, which is important information for governmental decisions about the designation of catastrophe zones, and about how to share and allocate risk [3, 4].

Risk-assessment models are generally made up of four modules: hazard, vulnerability, exposure, and damage [2]. When dealing with windstorms, such as hurricanes and typhoons, the first module's hazard values represent their intensity in terms of wind speed, while its hazard curve indicates the probability of particular wind-speed values occurring. The vulnerability module estimates damage potential as a function of the intensity of the hazard; the exposure module provides information about the properties that may be affected; and the damage module estimates the total loss [5]. This implies that it is critically important for the exposure module to incorporate detailed information regarding properties, such as their building materials, heights, numbers of floors, ages, and locations, if accurate evaluations of damage and losses are to be obtained. However, such property information at a regional scale is often incomplete, or of a poor quality, leading to inaccurate risk-assessment modeling results, which in turn can hinder governmental and insurance-company efforts to plan for disasters.

An alternative approach makes use of post-event data: specifically, the claim payouts determined by engineers and adjusters from insurance companies, which is a relatively reliable index of loss. Vulnerability curves for buildings subjected to high winds have been developed based on such post-event loss data, and are arguably a more reliable way to assess building damage caused by windstorms than any other existing method [5]. Vulnerability curves are generally presented in the form of vulnerability functions that express the correlations among damage ratios, wind speeds, and damage states [6]. According to Jaimes et al. [7] and Goyal and Datta [8], damage can be represented as the ratio of the expected repair cost of each structure to its total construction cost. Insurance-company data on financial losses can also be used to represent damage. Kim et al. [9] and Ahn et al. [10], for example, computed damage ratios by dividing claims payouts for repair costs to particular buildings by the total construction cost of those buildings. As well as being objective, this quantitative approach has the advantage of capturing the *extent* of damage, regardless of structures' sizes or construction budgets. And in practice, it can be assumed that a low damage ratio equates to low vulnerability. However, effective use of damage ratios requires that researchers define damage states. Goyal and Datta [8], for instance, defined damage states as the failure of specific components (e.g., various types of walls, roofing material, roof members, roof members' connections to walls) at particular wind speeds; and overall damage as the combination of all such failures. By its nature, however, such an approach requires much more detailed damage and wind-speed information than is commonly available.

As a proof-of-concept, the present study develops vulnerability curves pertaining to the high winds of Typhoon Maemi in South Korea in 2003, using actual loss data from a local insurance company (Figure 1). Damage ratios and damage states are utilized to assess the vulnerability of each insured property at particular recorded wind speeds during that catastrophic event. Specifically, damage ratios were established by dividing the insurance-claim payout amount by the total value of the insured property. Damage states, meanwhile, were defined according to the correspondence between damage-ratio distribution and five wind-speed intervals, i.e., 10.00-14.99 meters per second (m/s), 15.00-19.99 m/s, 20.00-24.99 m/s, 25.00-29.99 m/s, and 30 m/s and above. This resulted in the identification of four damage states, ranging from 0 to 0.01, i.e., 0-0.00299 (state I); 0.003-0.0059 (state II); 0.006-0.0099 (state III); and 0.01 (state IV). This data formed the basis of a damage matrix, from which the vulnerability curves of each damage state were computed. Then, damage data from Typhoon Maemi in 2003 were utilized to show how well each vulnerability curve predicted financial damage ratios. This study's procedures and findings

should be useful references for government, insurance-industry, and construction-industry personnel who need to assess the relationships between structural damage to buildings and the intensity of windstorms.

2. Literature review

2.1 Prior studies involving vulnerability to wind

The history of wind-damage modeling can be traced back nearly half a century. Friedman [11] proposed a model that classified undamaged and damaged buildings, with data on the former being utilized to estimate the probability of damage as a function of wind speed, and the latter, the probability of particular damage ratios, again as a function of wind speed. Leicester and Reardon [12] developed their model based on observed damage states to typical single-family houses when Cyclone Tracy struck Darwin in 1974. Hart [13] proposed an engineering-based vulnerability model to estimate the risk of damage to buildings from tornadoes, using experts' judgments of damage states as a function of wind speeds where the damage occurred. And Sparks and Bhindarwala [14] studied the existing vulnerability models for typical single-family houses in Florida, in light of an insurance company's records of damage and losses from Hurricane Andrew, and used the results to create a model of economic impacts that could be used in disaster mitigation.

Khanduri and Morrow [5] developed vulnerability models for different types of buildings, using a large amount of real-world damage data. However, their modeling was not sufficient by itself to explain the vulnerability curves of individual building types. Vickery et al. [15, 16] later proposed a comprehensive vulnerability model, which included wind features such as hurricane wind speeds, and wind loads on particular building components, as well as engineering judgments. Henderson and Ginger [17] applied Vickery et al.'s [15, 16] model to typical houses in northern Australia, and estimated the probability of damage – and of certain damage states being reached – according to the various failure levels of such properties as a function of wind speed. Heneka and Ruck [18] focused more narrowly on the initial wind speeds that damaged buildings, as a parameter of vulnerability, and assessed the statistical features of winds of various speeds. Walker [19], however, argued that developing a universal vulnerability model is very difficult due to the lack of damage data on extreme events in some countries, as well as sharp international variation in building codes and construction quality. Walker therefore studied how insurance companies simulate wind-damage patterns, and found that in practice, the cost of repairing and replacing damaged buildings was the most common metric of wind damage. Specifically, a damage pattern was usually represented empirically by a plot of the maximum wind speed where damage repair costs were incurred against the damage ratios of the buildings in those places.

Insurance companies tend to recognize the value of catastrophe-loss modeling and use it widely in quantifying and allocating risk to specific types of structures within their portfolios. Usually, these companies' vulnerability models, and thus their vulnerability curves, have included information related to damage functions, such as each building's history of prior wind damage and other negative events, as well as its number of floors, occupancy class, location, and so forth. Watson and Johnson [20], for example, evaluated the combination of windstorm damage, vulnerability, and risk through wind models and damage models from previously published literature, and used their results to develop an enhanced type of loss-assessment modeling.

The exceedance probability for a given damage ratio is usually expressed as a function of wind speed, and different curves indicate different damage states. In other words, vulnerability curves show that the probability of exceeding a particular damage state is 0% up to a certain critical wind speed, i.e., the threshold determined by the damage ratio. Above that threshold, a property's probability of exceeding a particular damage state increases until, at a certain maximum wind speed ($v_{maximum}$; [6]), it reaches an exceedance probability of 100% – meaning that it has totally collapsed or is so severely damaged that it must be replaced rather than repaired. Those vulnerability curves that take account of wind speed and direction, as well as specific types of construction and the vulnerabilities of different infrastructure types, are extremely useful tools for predicting the possibility of reaching or exceeding different damage states [21]. Based on the above literature review, it is also clear that studies have hitherto used damage ratio, considered as a function of wind speed, as their main dependent variable. Friedman's [11] above-mentioned investigation of vulnerability curves for hurricane loss, for instance, involved placing contour maps of maximum wind speeds during actual disasters over the properties covered by a specific insurance company; and he later adapted this method to estimation of earthquake damage losses.

To estimate the vulnerability of rural housing, Goyal and Datta [8] considered wind directionality for the 16 orthants and components of each building, and arrived at failure velocities on a component-by-component basis according to where the wind was coming from [8]. Wind direction was revealed to have a significant effect on overall annual damage to rural housing, as well as a marked, but non-significant, effect on the scale of that damage. Similarly, Rhee and Lombardo [22] used tree-fall patterns during tornadoes, and Rankine vortex simulation of fallen-tree patterns, to approximate the near-surface wind fields of tornadoes and construct fragility curves, with the wider aim of providing guidelines for tornado-resistant structural design [22]. Event-based wind-risk damage assessments have also been proposed for protecting Mexican wind farms' turbine towers from tropical cyclones, by Jaimes et al. [7]. That study calculated average annual loss and probable maximum loss based on time-history analysis at various intensities of wind velocities and the turbines' various heights. The results were represented as a fragility function with three modes: i.e., residual displacement, yielding of the tower, and collapse.

Cui and Caracoglia [23] researched methodologies for assessing the lifetime costs of tall buildings along the U.S. Atlantic coastline, utilizing the representative concentration pathways published by the Intergovernmental Panel on Climate Change to acquire additional quantitative information. Hurricane simulation was introduced to estimate hurricane intensity and frequency at the various representative concentration pathways. The simulated tracks of hurricanes coupled with data on existing tall buildings were used to estimate the likely structural performance and lifetime damage/costs to such buildings of future hurricane-induced wind hazards. In place of risk assessment of independent assets, an interdependent risk-assessment methodology has been developed by Dunn et al. [24], based on catastrophe modeling (CAT) modeling not of individual properties, but of system resilience, taking account of the geographical distribution of properties in hurricane-prone areas. Specifically, their research utilized empirical data on damage to overhead electrical lines caused by high wind speeds and other storm hazards to construct and test the spatial resolution of fragility curves based on three distinct methodologies (i.e., high resolution, low resolution, and land use). The R^2 in Dunn et al.'s statistical analysis indicated that high spatial resolution had the greatest effect on the curves. The same study analyzed three major components of wind loading

on transmission towers – i.e., transverse wind load, longitudinal wind load, and wind load transferred from the wires – as represented by wind speed, wind angle, and horizontal length of the transmission lines. Kriging was then applied to identify the relation between the capacity surface of the transmission-line towers and structural uncertainty, based on the wind-load parameters.

Cai et al. [25] adopted Monte-Carlo simulation to estimate the possibility of the failure of towers as a result of extreme wind hazards. Suvanto et al. [26] used spatial data from forest mapping to investigate the probability of disturbance over a large area and a five-year timeframe, taking account of forest characteristics, return rates of wind speeds, soil conditions, and climate conditions. They used three different methods (i.e., boosted regression tress, generalized addictive models, and generalized linear models) to create their probability model. That probability model, along with three different models generated from damage-probability maps coupled with geographic information systems (GIS) data, yielded damage predictors of potential extreme wind hazards. A more reliable quantification method for uncertain wind-induced losses during various intensities and frequencies of storms was developed by Khajwal and Noshadravan [27], using nonstationary stochastic processed economic-loss modeling. Specifically, they used insurance loss data and tested a prediction model for estimating the loss caused by strong winds at a regional level.

Mitsova et al. [28] looked into the effects of hurricanes on power outages in Florida, using multiple regression analysis of power-outage data during the period of Hurricane Irma, and identified important differences between rural and urban areas in terms of power restoration, power-outage duration, and the relation between power outages and socio-economic vulnerability. They also identified Irma's wind field as one of the critical reasons for electric power outages in Florida during that hurricane. Another approach to assessing the structural vulnerability of buildings was made by Hatzikyriakou and Lin [29] who, rather than treating each natural hazard independently, computed joint natural-hazard return periods. Specifically, they first created synthetic storms crossing Manhattan Island, and then separately utilized the Holland gradient wind profile to simulate their wind speeds, and advanced circulation to simulate their storm surges. The resulting simulated wind speeds and surges of the synthetic storms were then used to arrive at the joint return periods of these two natural disasters, using bivariate copula and exceedance thresholds. Lastly, they used generalized Pareto distribution to fit the two natural hazards' return periods at particular target areas.

2.2 Prior studies of typhoon damage in South Korea

Previous research on damage caused by typhoons in South Korea has mainly focused on those storms' characteristics. For instance, Ku et al. [30] developed a prediction model using storm-induced rainfall data; Park et al. [31] and Park et al. [32] utilized data on typhoons' wind fields and highest wind speeds to predict the area and extent of the damage they caused; and Shin et al. [33] estimated property damage based on typhoons' movement speed and direction.

Kim et al. [34] identified hurricane wind speed, building age, and building floor area as key independent variables, and damage ratios as their dependent variable, based on Hurricane Ike-related claim-payout data from the Texas Windstorm Insurance Association. Through Spearman correlations, they found that maximum wind speed and

building age had a positive relationship with damage ratio, whereas building floor area had a negative relationship with it. However, that study was limited by its use of 1) only wind speed, from among the wide range of other hurricane characteristics; 2) damage data only from commercial buildings; and 3) only one case, Hurricane Ike. Kim et al. [4] studied the same data, but applied more independent variables, including appraised building value, surge zone, side of hurricane track, and distance from shore. They found that building value and being on the right-hand side of the hurricane track both had positive relationships with damage ratio, whereas for surge zones and distance from shore, these relationships were negative. Like Kim et al. [34], however, their study focused solely on commercial property damage and Hurricane Ike, and thus was not a sufficient basis from which to generalize vulnerability as a function of typhoon wind speeds across the numerous different types of buildings and building materials that can be found around the world.

Another approach to predicting and estimating damage was investigated by Kim et al. [35], who categorized typhoons affecting the Korean Peninsula, and then used these categories to estimate property vulnerability. Specifically, typhoons that made landfall on the west coast of the peninsula were classed as Type 1, and those that struck its southern coast as Type 2. Loss ratio was used as the dependent variable, while the independent variables were rainfall, radius, maximum wind speed, forward movement speed, and the number of hillside and mountainside areas whose slope-angles had decreased due to urban or agricultural development. The authors concluded that the extent of damage caused by Type 1 typhoons was correlated, in descending order, with maximum wind speed, decreased slope, and rainfall. The critical damage indicators for Type 2 typhoons, in contrast, were – again in descending order – forward movement speed, rainfall, maximum wind speed, and radius. In short, differences linked to different landfall locations can have profoundly different impacts on storm-hit communities.

2.3 The relation of typhoons' characteristics to the extent of damage they cause

As the above discussion suggests, the severity of typhoons can be measured in various ways, including their maximum wind speed, peak wind duration, wind radius, speed of forward motion, and motion direction [15, 36, 37]. Several studies have linked the extent of property damage to one or more such characteristics, with some researchers having argued that maximum wind speed and maximum wind radius are the most critical factors in this regard [15, 36]. Others have posited that forward-motion speed is the most important variable, due to its impact on flood volume: with slow-moving typhoons likely to cause more property damage due to heavy flooding than their fast-moving counterparts do [38]. According to Choi and Fisher [39], rainfall is another key variable in determining the extent of damage; and the characteristics of the built environment, typhoon frequency, and other factors have also been proposed as key to effective windstorm-damage assessment [4, 5, 40]. In the present study, 10-minute maximum sustained wind speed has been used to construct the vulnerability function, since wind speed has long been the most commonly accepted means of classifying typhoons' and hurricanes' strength.

The U.S.'s National Oceanic and Atmospheric Administration coordinates a hurricane-observation system that provides its Hurricane Research Division with real-time wind analysis at 4-6 hour intervals during hurricanes. The collected wind data includes each storm's maximum wind speed, its forward movement speed and direction, and its winds' direction and duration [37, 41, 42, 43]. This information, especially when combined with GIS spatial data, can be applied effectively to classify hurricanes.

Built-environment vulnerability is also regarded as a critical factor in the damage caused by typhoons [4, 5, 44]. Khanduri and Morrow [5], for example, have suggested that high-rise buildings are likely to incur more damage than other structures; and, as noted above, decreases in the slopes of mountains due to urban or agricultural development have also been associated with the extent of damage caused by major storms [45, 46, 47, 48].

Another important factor in existing methods of assessing damage caused by typhoons is a given property's position in relation to the storm. In the northern hemisphere, the right-hand side of hurricanes generally causes more damage than the left-hand side. This is because storms' counterclockwise direction of rotation multiplies their winds' intensity and speed on that side [49, 50].

2.4 Use category, construction typology, and contents

Vulnerability curves that are appropriate to use in the insurance industry also take account of *line of business*, i.e., groupings of buildings or other properties according to similarities in their uses and property policies. Within the field of civil engineering, however, the same term is applied to groupings of buildings according to their structure, use, and resale values. Thus, the three most commonly used lines of business within the latter field are industrial, commercial, and residential [2]. Most of the prior literature has focused on residential buildings, due to the abundance of loss data for them, as compared to the other two. However, the present study will combine all three of these lines of business to produce a more robust dataset.

It is possible to construct empirical vulnerability curves based on historical damage data for specified regions, without taking account of construction types, materials, loads, and so on [2]. Nevertheless, masonry walls differ from other walls in terms of the levels of damage they are likely sustain at a given wind speed [5, 51]. To account for such variation, empirical vulnerability curves can be combined with engineering-based ones that incorporate construction typologies such as region-specific and line of business-specific materials, structure types, and load types [2].

Arguably, it is useful to consider buildings' interior contents when creating vulnerability curves for them, since such contents can be damaged by high winds, and are generally covered by insurance policies. However, interior contents' contributions to total damage costs are very difficult to gauge and analyze; and at low wind speeds, such items only tend to be at risk from flood damage, not direct wind damage. Therefore, they have not been included in this study's calculations of damage ratios.

3 Research methods

In terms of recorded damage, Typhoon Maemi was the costliest in the history of South Korea. As of the time of writing, this storm and its two nearest rivals, Kompas and Bolaven, account for 85.7% of the total typhoon damage and 66% of the total typhoon casualties in South Korea's history [2]. Although Maemi impacted the entire country, the southern part of the Korean Peninsula was hit especially hard: with the city of Busan alone suffering 35% of South Korea's total damage costs, and 29% of its total of losses by number of properties destroyed. The main purpose of this research is to develop reliable empirical vulnerability curves for damaged properties, based on a Busan-based insurance company's large, high-quality set of loss data pertaining to Typhoon Maemi. Each curve

will be generated based on damage ratios, wind speed, and the above-mentioned damage states, i.e., I = Slight, II = Light, III = Moderate, or IV = Major.

In computation of the damage states for the vulnerability function in the present study, aleatory and epistemic uncertainty were both considered to be random uncertainty. Aleatory uncertainty has an inherent random nature, and is therefore not reducible. Epistemic uncertainty, on the other hand, arises from lack of sufficient knowledge (e.g., building type and structure type), and therefore can be reduced if, for example, new data becomes available [52, 53]. Uncertainty has been approached via evidence theory, possibility theory, and fuzzy-set theory. In the present study, evidence theory's monotone measure was applied to the damage data to reduce the uncertainty of the vulnerability functions, since that measure can be utilized to quantify uncertainty [54]. The monotone-measured damage ratios were assorted sequentially at each damage state with respect to the corresponding wind-speed interval. Also, at a given state of damage, the monotone measures were set at 1 or 0, depending on whether or not the monotone-measured damage ratio exceeded, or was less than, the wind speed. Epistemic uncertainty was also reduced through the use of high-quality damage data (i.e., from an insurer) pertaining to a relatively compact site (i.e., Busan).

Vulnerability functions model the probability of structures exceeding certain limits or states at a given wind speed. This approach can produce quantitative and objective determinations of how structural failure occurs. It was initially developed and used for earthquake-damage risk assessment, and is still mainly used in the field of seismic risk management. Basoz and Kiremidjian [55] developed curves using bridge-damage data from the Northridge earthquake in 1994, while Shinozuka et al. [56], Porter et al. [57], and Lin [58] developed curves for the vulnerability of structures to seismic loading. Recently, vulnerability curves have been widely used in the insurance industry for risk assessment and premium-setting related to natural disasters, including hurricane-induced damage [59]. However, the application of such curves to wind hazards has been limited, especially in the case of potential damage to infrastructure systems.

The vulnerability function was pioneered based on study of structures' components. Holmes [60] proposed curves based on the assumption that they could be estimated by the cumulative distribution function of the components. Pinelli et al. [61] estimated the repair costs of wind-induced damage using a similar component-based approach, as did Ellingwood et al. [59] in the case of wind and earthquake damage. In 2006, Li and Ellingwood [62] extended this previous research to low-rise wooden residential buildings, to establish a probabilistic framework for component damage in hurricane-prone areas. In the same year, Vickery et al. [16] proposed a damage-prediction model that utilized the HAZUS-MH hurricane model, again based on component vulnerability.

Wind-induced vulnerability functions have been developed by Sparks et al. [14], Huang et al. [40], and Khanduri and Morrow [5], and buildings' wind-induced hazard vulnerability curves have been investigated eagerly for more than a quarter of a century. Sparks [14] introduced and developed deterministic vulnerability functions based on the typical single-family dwellings that existed when and where Hurricane Andrew occurred. Katz [63] later utilized stochastic models, in which extreme storm events served as the extreme-value functions, and the Poisson process was utilized to model economic loss. Khanduri and Morrow [5] proposed vulnerability functions for a disaggregation of generic curves to different types of buildings; and the impact of the uncertainty of the damage

cost of hurricanes was investigated by Wang et al. [64]. CAT has been usefully applied to the quantification of risk, including from natural disasters [65], and is especially attractive because it can reduce the uncertainty of damage databases and economic losses associated with such hazards [24]. In addition to analytically based and performance-based vulnerability models, empirically based ones have been introduced recently, based on synthetic wind profiles [66]. And, as noted above, fallen-tree analysis has been introduced as an alternative methodology for estimating surface wind-field profiles [22].

The present study extends these previous efforts to estimate vulnerability to wind hazards by adding empirical monetary losses incurred by particular properties, an approach that can reasonably be expected to dramatically reduce uncertainty while also increasing objectivity (Figure 2). The data matrix described above was utilized for assigning a degree of belief in a binary damage response (1 or 0) to the different damage states associated with the selected wind-speed intervals. Based on the collected damage data, lognormal probability distribution and maximum likelihood were utilized to generate a vulnerability curve for each of the four damage states.

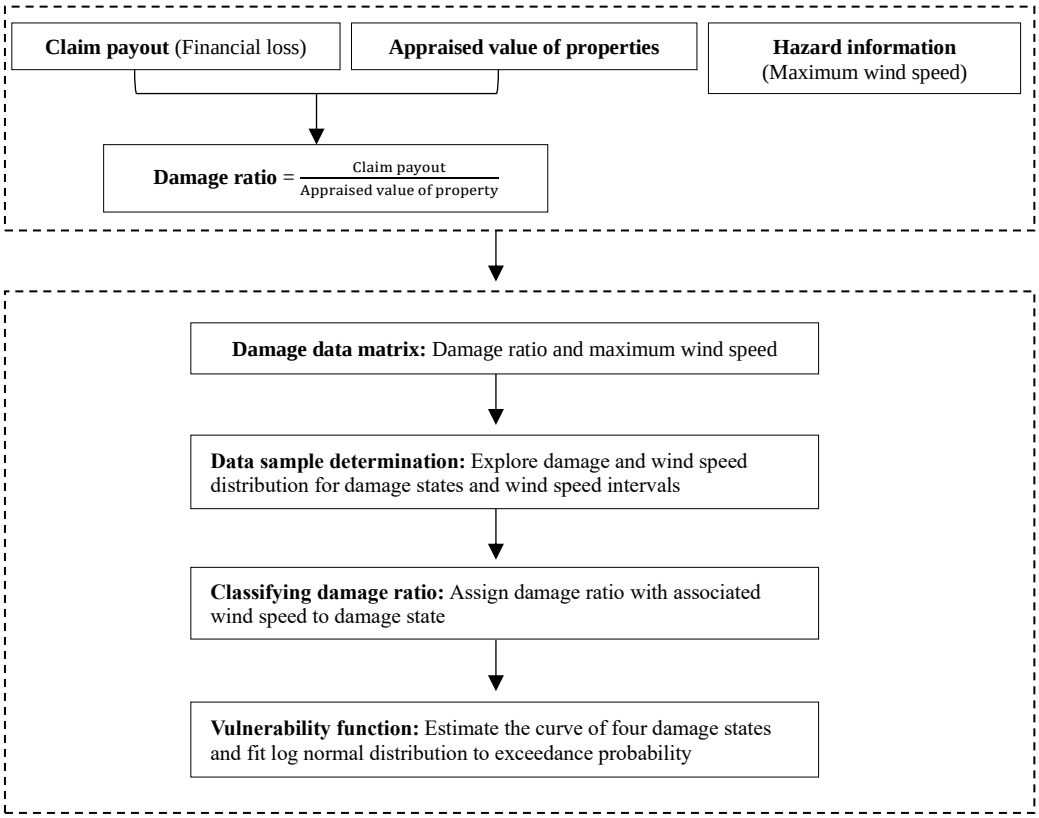

Figure 1. General approach and workflow

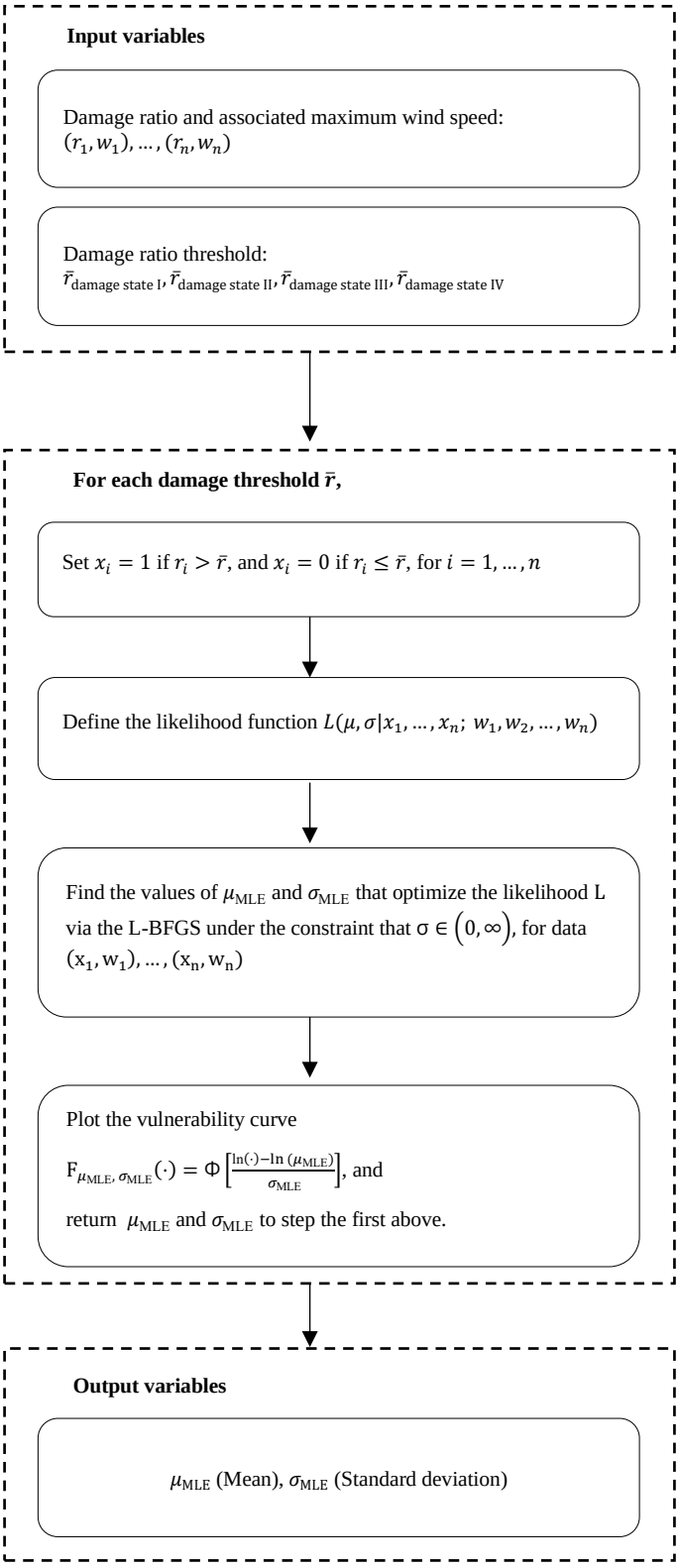

Figure 2. Workflow of vulnerability model

3.1 Case study of windstorm-induced damage

3.1.1 Study area

Busan has a population of 3.5 million people, plus another 4.5 million in its wider metropolitan area, and is located in the southeast of the Korean Peninsula. Thanks to this location, its international trade has boomed, and as a consequence, it has the largest port in South Korea. The longest and widest river in the country, the Nakdong, also passes through it. Due to these geographical characteristics, Busan has been very vulnerable to typhoons and other storms, and the importance of accurately predicting the impact of future storms on it has been increasingly recognized by government agencies and other stakeholders. In Figure 3, the white line indicates the boundary of Busan, and the yellow line, the track of Typhoon Maemi. The damage ratios for each insured property are shown in Figure 5, with differently sized circles indicating different extents of damage.

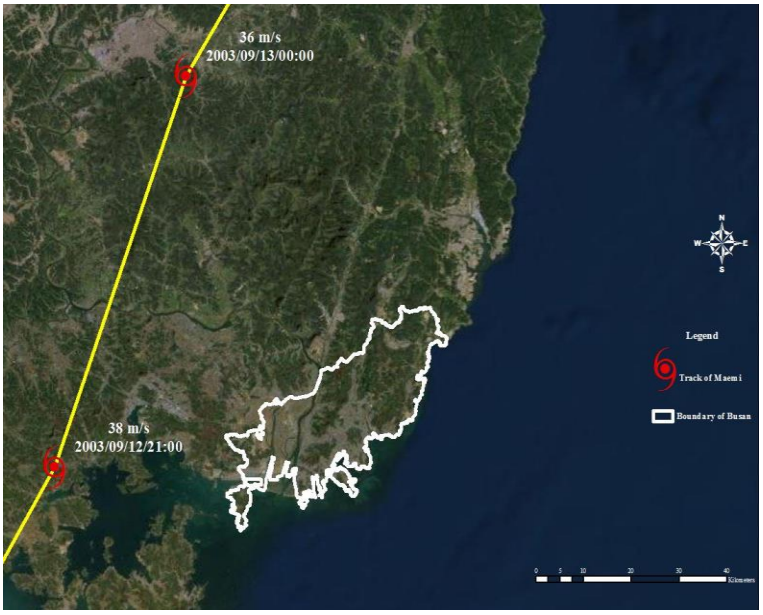

Figure 3. Track of Typhoon Maemi

3.2 Data collection

In addition to the Typhoon Maemi loss dataset, this study utilizes data on 10-minute sustained maximum wind speeds provided by the Korea Meteorological Administration. Critical information such as the address, damage losses, and value of each insured property has been extracted from the insurance-company dataset. The original, Korean-language data have all been translated into English. GIS has been used to record the longitude and latitude of each property, and to construct a map that includes its damage state and wind-speed exposure history.

3.3 Data analysis

3.3.1 Damage-ratio computation

A statistical model was developed to construct vulnerability curves for wind-induced damage. As noted above, the main purpose of such curves is to indicate the probabilities of particular damage states as functions of various wind speeds.

A damage ratio for each component was established to facilitate quantitative, objective assessment of the damage caused by the focal typhoon. While other researchers [9, 10] have used total construction cost or total insured amount of projects, the present study utilizes both the total value of insured each property and the damage-claim payout amounts arising from Hurricane Maemi to estimate damage ratio for vulnerability curves as a function of the wind speed. Such an approach can aid understanding of the extent of the damage, regardless of the amount of loss or the size of the building. Here, a damage ratio is defined as the ratio of the financial loss to the total value of insured property, as shown in Eq. (1), below:

$$\text{Damage Ratio} = \frac{\text{Claim payout}}{\text{Total value of insured property}} \tag{1}$$

The damage ratios of properties in Busan affected by Typhoon Maemi ranged from 0 to 0.01, with higher damage ratios indicated more damage, greater financial losses, and at least by implication, higher vulnerability to typhoons.

3.3.2 Spatial distribution of damage

Wind speed at the location of each property was calculated in ArcGIS (Esri, Redlands, CA) using its inverse distance weighted tool. This yielded an enhanced dataset that includes maximum sustained wind speed and direction, as well as gridded data, image data, and GIS shape files, all of which are essential information for constructing an ArcGIS wind map like Figure 4. More specifically, a wind map of typhoon damage relies on the interpolation of wind-speed data pertaining to each damaged property with the maximum 10-minute sustained wind speed at each wind-observation station. Different wind speeds and wind directions (wind angles) in Figure 4 are indicated by color (with green representing the slowest, and red the fastest) and contour. Each property's location, based on the longitude and latitude provided by the insurance company, and the extent of its damage, are also marked on the map in Figure 5.

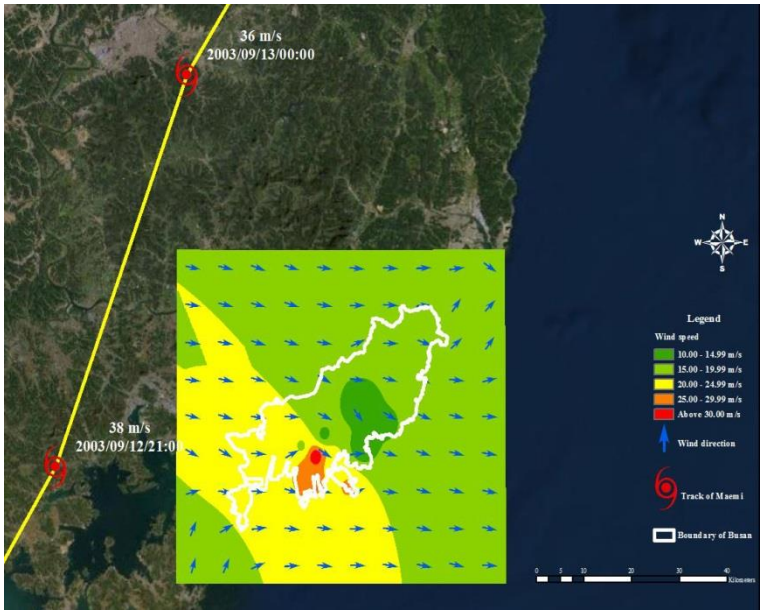

Figure 4. Wind-speed map with spatial distribution of damage

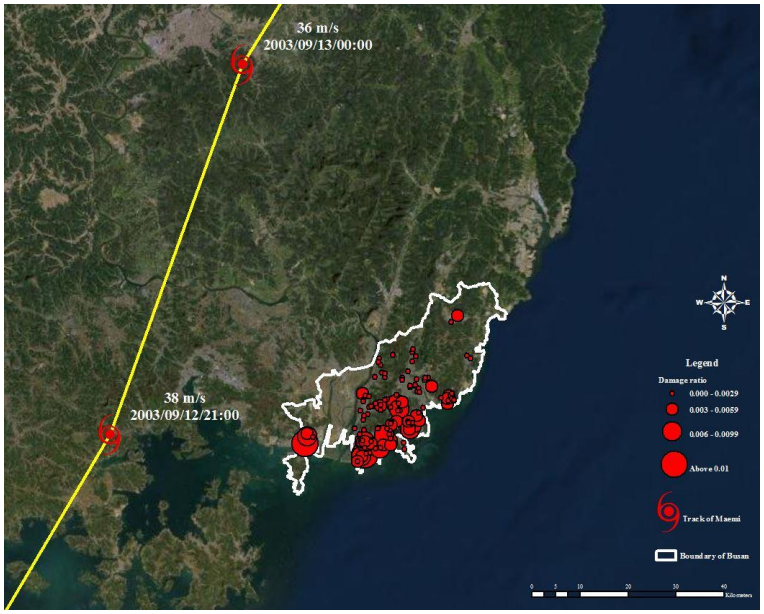

Figure 5. Spatial distribution of damage

4 Data-analysis results

In all, 126 observations of damage ratios and related maximum wind speeds were made, i.e., 90 of residential buildings, and 18 each of commercial and industrial buildings. The present research modeled vulnerability curves of the analytical type using the cumulative distribution function of the lognormal distribution, and then estimated four distinct vulnerability curves, each with its own damage threshold ranging from damage state I to damage state IV. Two different approaches were used for such estimation: the first based on mean square error (MSE), and the other on maximum likelihood estimation (MLE). Each approach is described in turn below.

4.1 Mean squared error method

Assume that n damage ratios $r_1, r_2, \ldots, r_n$ are observed, along with their associated maximum wind speeds $w_1, w_2, \ldots, w_n$, and that the former are assigned to groups based on the latter. For each such group, the fraction of ratios that exceed a given wind-speed threshold is computed, and serves as an observation of the vulnerability curve of interest at that point. As well as their maximum wind speeds, all damage ratios are grouped according to the five wind-speed intervals described in introduction section, above. Each wind-speed interval contains all four of the damage states described in introduction section, above; and for each such damage state within each wind-speed interval, a damage ratio is computed. The numbers and percentages of the damage ratios that are equal to or larger than each damage state within each wind interval are shown in Table 1 and Figure 6.

Table 1. Numbers and percentages of damage ratios, by wind-speed interval

Wind-speed interval (m/s) / Frequency of damage ratios	10.00-14.99 m/s	15.00-19.99 m/s	20.00-24.99 m/s	25.00-29.99 m/s	30.00 m/s or above
Number of damage ratios (≥damage state I)	8	50	30	35	3
Number of damage ratios (≥damage state II)	6	34	19	26	3
Number of damage ratios (≥damage state III)	3	18	12	19	2
Number of damage ratios (≥damage state IV)	3	13	10	14	2
Percentage at damage state I (%)	100	100	100	100	100
Percentage at damage state II (%)	75	68	63	74	100
Percentage at damage state III (%)	38	36	40	54	67
Percentage at damage state IV (%)	38	26	33	40	67
Total number of damage ratios	8	50	30	35	3

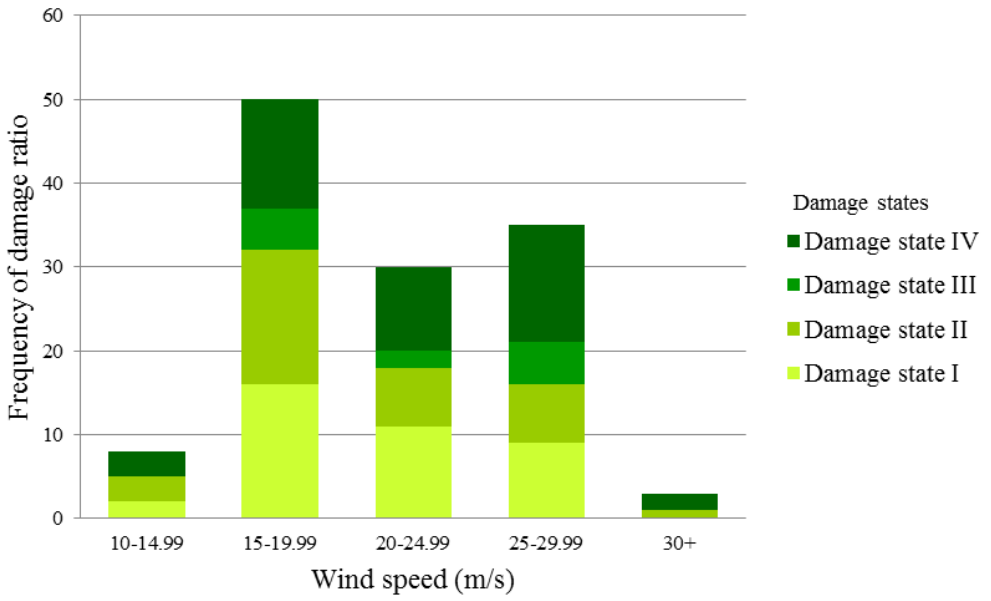

Figure 6. Number of damage ratios per wind-speed interval

For example, all damage ratios whose associated wind speed was at least 15 but less than 20 m/s were assigned to damage state II. By dividing the number of damage ratios equal to or larger than damage state II in that wind-speed interval by its total number of damage ratios, we arrive at a figure of 0.68, indicating that 68% of these ratios are above the threshold for damage state II, and therefore, that the probability that damage state II will be exceeded within that wind-speed interval is 68%. When calculating the vulnerability curve for damage state II at any average maximum wind speed within the same interval, 68% can thus be used as the percentage of damage ratios; and the same method can be applied to the curves for damage states I, II, III, and IV. Figure 7 presents plots of the exceedance probabilities of each damage state in each wind-speed interval.

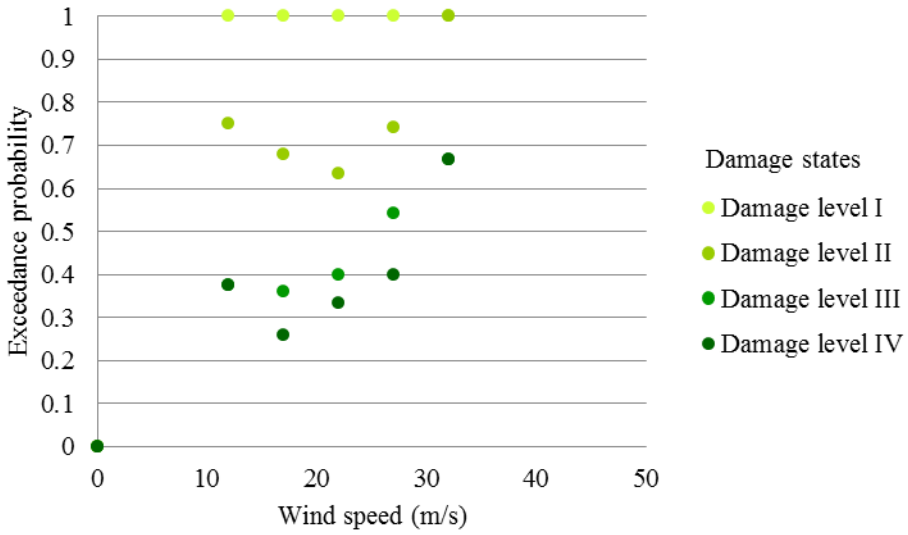

Figure 7. Exceedance probability of damage states, by wind speed interval

Following the above approach produces m realizations $p_1, \dots, p_m$ (with $m < n$) of the vulnerability curve for given wind speeds $\bar{w}_1, \bar{w}_2, \dots, \bar{w}_m$. These realizations are estimated by finding the lognormal curve that minimizes the MSE with respect to $p_1, \dots, p_m$. Because each lognormal curve is univocally identified by two parameters, μ and σ, this amounts to finding the values of those parameters that minimize the MSE: i.e.,

$$\text{Min} \sum_{j=1}^{m} \left(F_{\mu,\sigma}(\bar{w}_j) - p_j\right)^2, \tag{2}$$

where $F_{\mu,\sigma}(w_j)$ is the lognormal cumulative distribution function with the following parameters:

$$F_{\mu,\sigma}(w_j) = \Phi\left[\frac{\ln(w_j) - \ln(\mu)}{\sigma}\right] \tag{3}$$

The resulting algorithm, *Mean squared error estimation of vulnerability curves*, is described in more detail below.

(1) Input: Data $(r_1, w_1), \dots, (r_n, w_n)$

Damage thresholds: $\bar{r}_{\text{damage state I}}$, $\bar{r}_{\text{damage state II}}$, $\bar{r}_{\text{damage state III}}$, $\bar{r}_{\text{damage state IV}}$

Representative wind speed per group: $\bar{w}_1, \bar{w}_2, \dots, \bar{w}_m$ (midpoint values)

(2) Output: $\mu_{\text{MSE}}, \sigma_{\text{MSE}}$

(3) For each damage threshold $\bar{r}$, do the following:

1) Assign each damage ratio x_i to a group based on its wind speed w_i
2) For each group j, compute the fraction p_j of damage ratios that are above $\bar{r}$
3) Find the values of μ_{MSE} and σ_{MSE} that minimize the MSE of the vulnerability curve $F_{\mu,\sigma}(\cdot)$ from $p_1, \dots, p_m$ and at the representative wind speed values $\bar{w}_1, \bar{w}_2, \dots, \bar{w}_m$
4) Plot the vulnerability curve $F_{\mu_{\text{MSE}}, \sigma_{\text{MSE}}}(w_j) = \Phi\left[\frac{\ln(w_j) - \ln(\mu_{\text{MSE}})}{\sigma_{\text{MSE}}}\right]$, and return μ_{MSE} and σ_{MSE} to step 1) above.

However, as shown in Figure 8, below, calculating vulnerability curves using the MSE method has limitations when it comes to explaining the correlations between those curves, for two reasons. First, the curves overlap at low wind speeds. And second, they do not show the exceedance probability for damage state I: instead, increasing continuously as shown in Figure 9, implying that some properties might not collapse even in a wind of 200 m/s: nearly double the highest speed ever recorded on Earth.

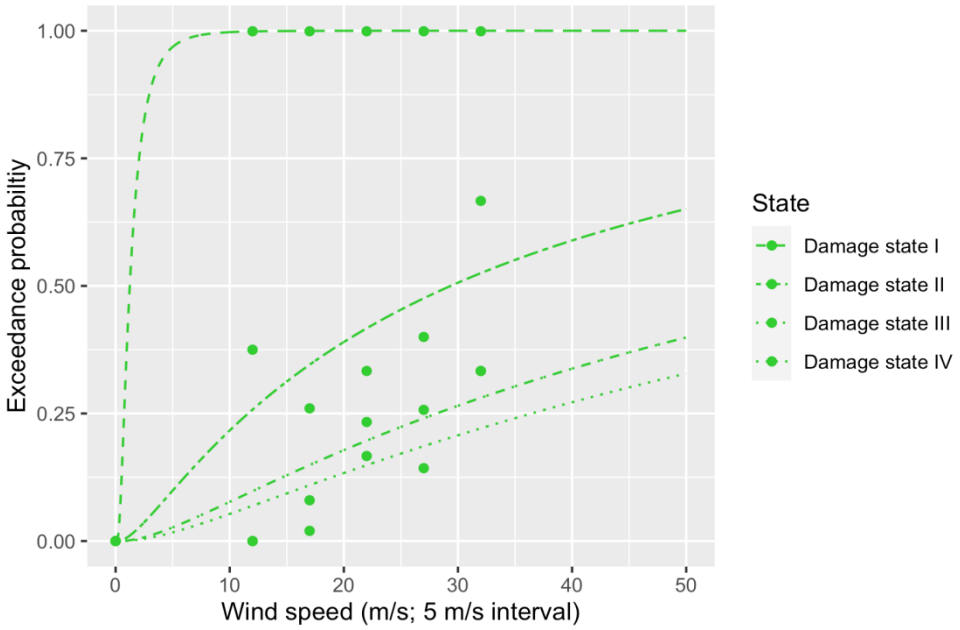

Figure 8. Vulnerability curves simulated by mean squared error, wind speeds of 0-50 m/s

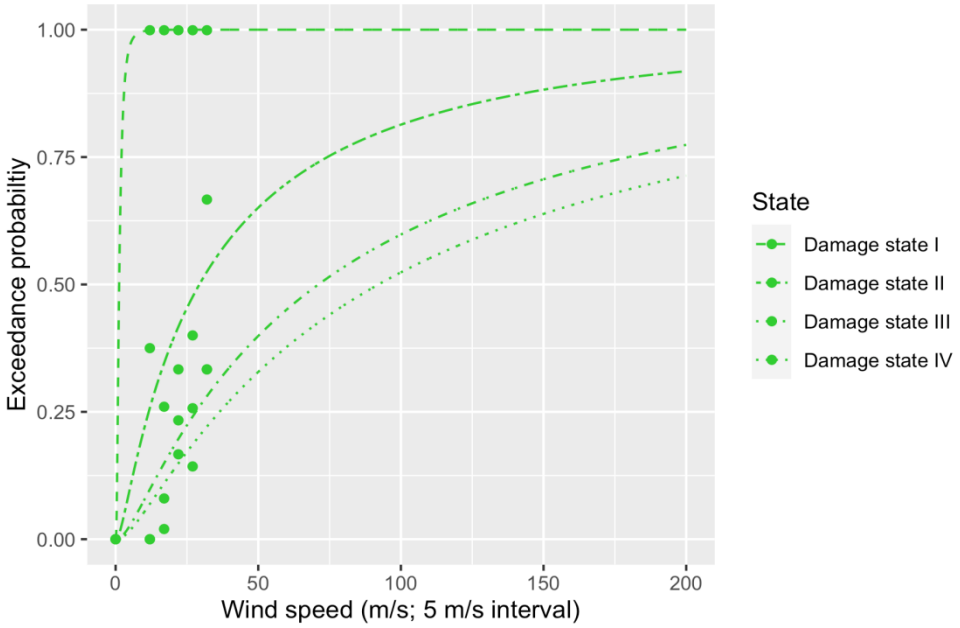

Figure 9. Vulnerability curves simulated by mean squared error, wind speeds of 0-200 m/s

4.2 Maximum likelihood estimation method

Given a family of distributions indexed by certain parameters, MLE can be used to select the parameter values under which certain data are most likely to be observed. Here, the same damage states used in MSE are used in MLE. A median of each damage-level interval is selected as the threshold: i.e., 0.0015 for damage state I (0-0.00299), 0.0045 for damage state II (0.003-0.00599), and 0.08 for damage state III (0.006-0.0099); while 0.01 is

used for damage state IV (as variations in its numerical value are not associated with any real-world damage differences). For the purposes of this study, MLE involves choosing the parameters that define the lognormal shape of the vulnerability curve by maximizing the likelihood function for the given data. To do that, a probability model for the data-generation process is specified. This model assumes that, for each incident of damage, n boolean outcomes $x_1, \dots, x_n$ are observed; and such outcomes indicate whether the damage is at least moderate or not. Hence,

$$x_i = \begin{cases} 1, & i\text{-th damage is at least moderate;} \\ 0, & \text{otherwise.} \end{cases} \tag{4}$$

Assuming that the maximum wind speed $(w_1, w_2, \dots, w_n)$ associated with each damage state can also be observed, then – following Shinozuka et al. [56] – the likelihood function can be built as

$$L(\mu, \sigma | x_1, \dots, x_n;\ w_1, w_2, \dots, w_n) = \prod_{i=1}^{n} \left[F_{\mu,\sigma}(w_i)\right]^{x_i} \cdot \left[1 - F_{\mu,\sigma}(w_i)\right]^{1-x_i} \tag{5}$$

where $F_{\mu,\sigma}(\cdot)$ is the vulnerability curve under the lognormal assumption, as previously defined.

The present study estimates each vulnerability curve by finding the values of the lognormal parameters μ_{MLE} and σ_{MLE} that maximize the likelihood function given above for data $(x_1, w_1), \dots, (x_n, w_n)$. For example, this could be achieved by numerically solving the resulting first-order conditions:

$$\frac{d}{d\mu} L(\mu, \sigma | x_1, \dots, x_n;\ w_1, w_2, \dots, w_n) = \frac{d}{d\sigma} L(\mu, \sigma | x_1, \dots, x_n;\ w_1, w_2, \dots, w_n) = 0. \tag{6}$$

In practice, this study directly optimizes likelihood via the limited-memory Broyden-Fletcher-Goldfarb-Shanno algorithm (L-BFGS) in R (R Foundation for Statistical Computing, Vienna, Austria). As with the MSE approach, this process is repeated for each level of damage, yielding four different vulnerability curves. Using observed damage ratios $r_1, r_2, \dots, r_n$ together with observed wind speeds $w_1, w_2, \dots, w_n$, Shinozuka et al.'s [56] algorithm *Maximum likelihood estimation of vulnerability curves* implements this method.

The present research is believed to be the first to use simulated data to test the validity of an implementation of Shinozuka et al.'s [56] MLE method for vulnerability curves. To generate this synthetic data, wind speeds were simulated first, as $\widetilde{w}_i = 13\ \text{m/s} + 0.1 * i$ for $i = 0, \dots, 30$, so as to obtain speeds that were equally spaced at plausible intervals (e.g., 13 m/s, 16 m/s). Next, the damage associated with each such wind speed was generated using the simple linear model $\widetilde{D}_i = \widetilde{w}_i + \varepsilon_i$, where ε_i is an error that follows a standard normal distribution. Hence, for each i, a random-draw ε_i was sampled from a standard normal distribution and then added to $\widetilde{w}_i$ to compute damage $\widetilde{D}_i$. Finally, the simulated damage ratios were computed by standardizing the simulated damage, by 1) computing the standard deviation σ_{obs} of the observed (i.e., non-simulated) damage ratios, and finding the smallest observed damage ratio DR_{min}; 2) computing the standard deviation σ_{sim} of the simulated damage ratios $\widetilde{D}_0, \dots, \widetilde{D}_{30}$ and finding the smallest simulated damage ratio $\widetilde{D}_{min}$; and 3) for each i, generating the i-th simulated damage ratio $\widetilde{DR}_i$ as:

$$\widetilde{DR}_i = \frac{\sigma_{obs}}{\sigma_{sim}} \cdot \left(\widetilde{D}_i - \widetilde{D}_{min}\right) + DR_{min}. \tag{7}$$

The normalization in the last step of the procedure above ensures that the simulated damage ratios preserve the observed variance of the real ones, i.e., from 0 to 1. After data simulation as described above, the simulated damage ratios were classified into four damage states, based on the following thresholds: below 0.005 for state I, between

0.005 and 0.01499 for state II, between 0.015 and 0.02499 for state III, and between 0.025 and 0.035 for state IV. For each damage state, Shinozuka et al.'s [56] MLE approach was then used to fit a lognormal vulnerability curve to the data, $(\widetilde{w}_i, DR_i)_{i\geq 1}$. The resulting vulnerability curves captured the simulated data as desired, and are plotted in Figure 10.

Finally, this study ran the same fit using real wind speeds w_i, and based on the results, set more suitable thresholds for the damage ratios. The curves that were fit on the fully empirical data are plotted in Figures 11 through 14.

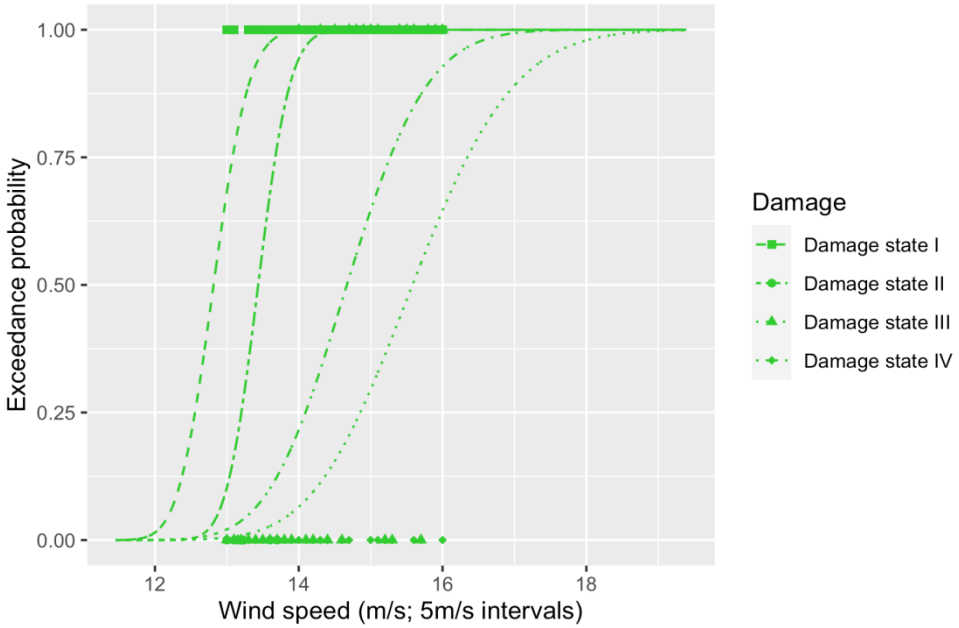

Figure 10. Vulnerability curves simulated according to Shinozuka et al.'s [56] method

The vulnerability curves based on the 2003 Typhoon Maemi data were computed following the likelihood function proposed by Shinzuka et al. [56], i.e.,

$$L = \prod_{i=1}^{N} [F(a_i)]^{x_i} [1 - F(a_i)]^{1-x_i} \tag{8}$$

where $F(\cdot)$ represents the vulnerability curve for a given level of damage; a_i is the wind-speed value, within which i represents the number of damage ratios; x_i = 1 or 0, depending on whether the damage ratio reaches/exceeds (1) or fails to reach (0) the level of damage under a_i; and N = the total number of damage ratios. Under the prevailing lognormal assumption, $F(a)$ takes the analytical form

$$F(a) = \Phi \left[\frac{\ln \left(\frac{a}{c} \right)}{\zeta} \right] \tag{9}$$

in which a represents the wind speed and $\Phi[\cdot]$ is the standardized normal distribution function. The two parameters c and ζ in Eq. (9) are computed as c_e and ζ_e, satisfying the following equation to maximize $\ln L$, and hence L:

$$\frac{d \ln L}{dc} = \frac{d \ln L}{d\zeta} = 0 \tag{10}$$

5 Discussion

As mentioned earlier, vulnerability curves provide the probabilities of a particular property reaching or exceeding specific damage states, as a function of wind speed, and taking account of 1) damage-level definitions; 2) the value of the insured property; 3) any payout claim pertaining to that property; and 4) Typhoon Maemi wind speeds at all property locations. The vulnerability curves computed as part of this study show that the probability of each damage state rests at 0, but once the threshold of a particular damage ratio is met, exceedance probability as a function of wind speed moves asymptotically toward a probability of 100%. The vulnerability curves plotted in Figures 11 through 14, below, show the exceedance probability of four different damage states as a function of wind speed (up to 200 m/s).

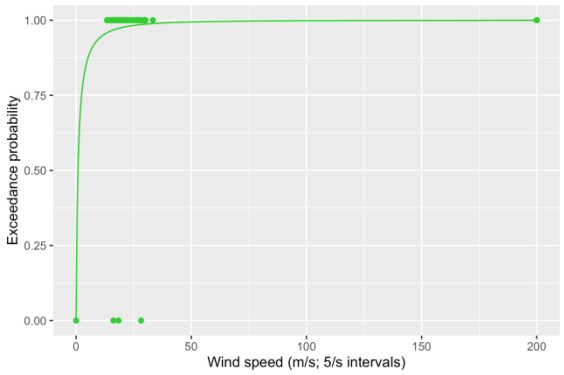

Figure 11. Vulnerability curve, damage state I

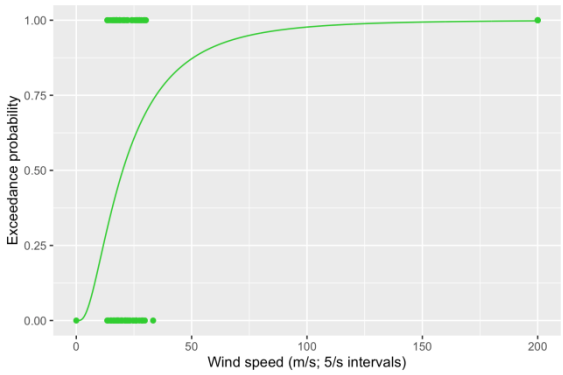

Figure 12. Vulnerability curve, damage state II

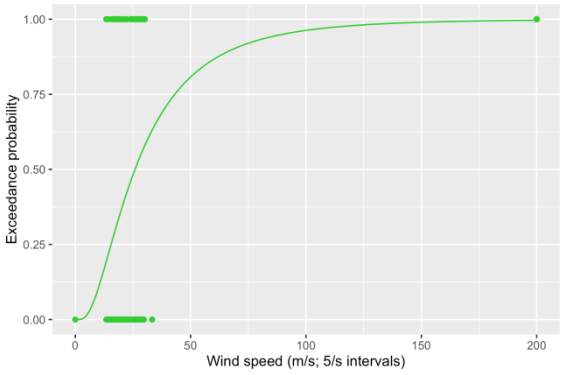

Figure 13. Vulnerability curve, damage state III

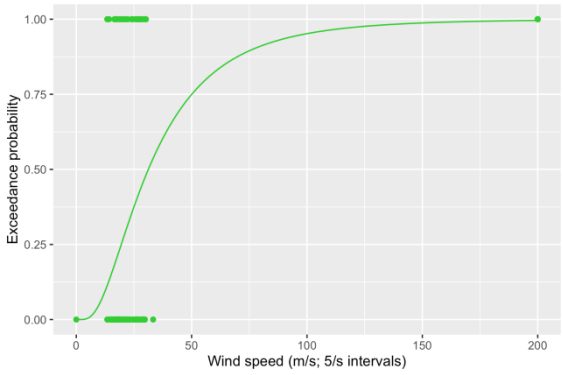

Figure 14. Vulnerability curve, damage state IV

Figure 15, below, illustrates the vulnerability curves for damage states I through IV side by side. The curve for damage state I indicates the probability of a property suffering at least damage state I at each wind speed a_i.

Each dot plotted at the top of the horizontal axis means x_i = 1, i.e., that such a level of damage will be reached or exceeded under a_i; while each dot plotted at the bottom means x_i = 0, i.e., that it will *not* be reached under a_i.

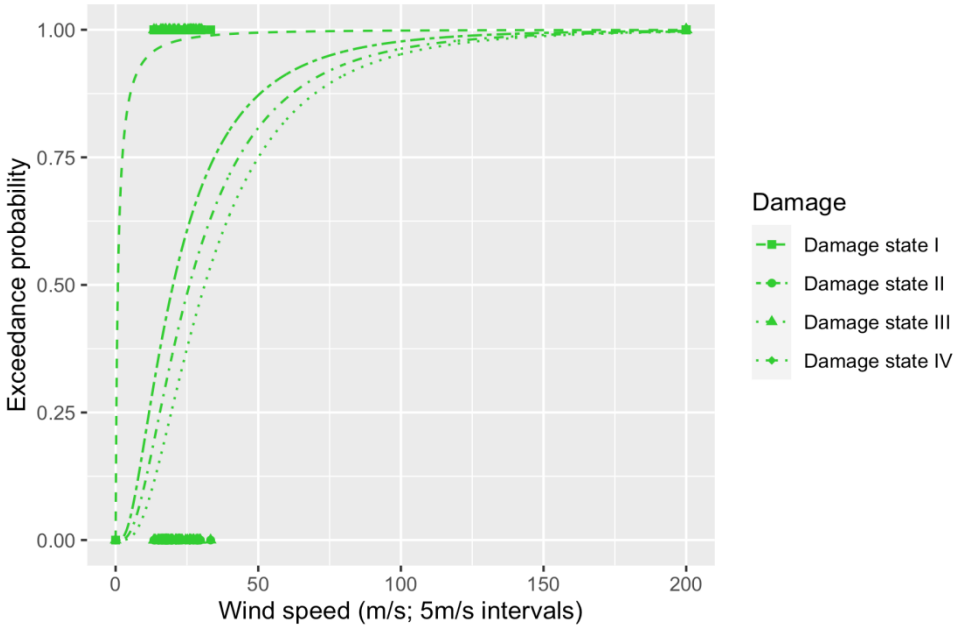

Figure 15. Vulnerability curves, damage states I through IV

6 Conclusion

To effectively plan for extreme weather events, governments and the insurance industry need accurate estimates of infrastructure's vulnerability to storms. This study has used wind speed-induced damage data provided by an insurance company in South Korea, in combination with empirical meteorological data, to develop vulnerability curves. Those curves' exceedance probabilities were shown to be capable of predicting the damage states to properties in Busan caused by various wind speeds during Typhoon Maemi. This approach represents a considerable advance over prior ones that primarily used damage judgments by experts, which are innately subject to considerable bias [24, 25]. To overcome that drawback, some previous research on windstorm-induced damage focused on variables related to other storm features such as wind direction and surface wind profiles [22]; environmental factors such as fallen trees [26]; and hypothetical data such as the paths of synthetic typhoons [23].

The present study's novel framework for vulnerability functions took account of the non-specificity of 126 cases of financial-loss data pertaining to Typhoon Maemi damage using statistical vulnerability modeling. Specifically, the financial-loss data was utilized in the form of ratios, which allowed for estimation of the extent of damage to a given property regardless of its size or value [9]. A binomial method for generating the vulnerabilities from the damage data was applied, and wind-speed data was classified into four different damage states based on damage-state evidence. In its first part, the present study investigated the exceedance probability of damage using an approach based on MSE, but found that the vulnerability curves for damage ratios continued increasing beyond wind speeds of 200 m/s, indicating that the methodology was not appropriate to estimating wind-induced damage. In its

second part, the vulnerability functions were expressed in the form of two parameters (i.e., log-standard deviation and median), using an MLE method that has been widely used to estimate seismic impacts on buildings. For this purpose, wind speed was used in place of peak ground acceleration to represent the associated damage ratio. Based on the occurrence of damage states within each wind-speed interval, the binomial of damage was assigned to the sets of damage states. The identified exceedance probabilities show that the possibility of damage states at a given wind speed differed very considerably from one building to another; and that wind speed had an important effect on wind-induced damage, supporting previous studies' findings [15, 16, 20, 36]. The vulnerability curves presented in the current study also show clearly that the extent of loss increases as maximum wind speeds increase.

Extreme winds cause major property losses all over the world. The empirical vulnerability curves calculated as part of this study have shown that, even if the line of business of damaged buildings is not considered, claim-payout and total insured value data for each property are sufficient to the calculation of damage ratios. As discussed in previous sections, the damage ratios from Typhoon Maemi can be separated into four damage states, each closely associated with a particular wind speed, as computed using MLE. The vulnerability curves can also explain exceedance probabilities at various wind speeds and various damage ratios. From the foregoing comparison of two estimation models, MSE and MLE, it can be concluded that lognormal distribution-based MLE was the more appropriate of the two, as indeed was previously shown in the case of earthquake-damage prediction [57, 58]. Though some calibration may be required, the present study's well-defined, efficient and simple probabilistic model for the estimation of natural hazard-induced financial loss can be used as a broad frameworks for risk-assessment decision-making, not only in Korea but in other regions with similar sizes of properties and similar wind-speed intensities. Most of the typhoon-related research in South Korea has focused on linking sizes and types of damage to specific typhoon characteristics [30, 31, 32], which places the present research in a class of its own. It is hoped that its promising new approach will be followed up by other researchers.

The findings of the present research also represent an opportunity for reconsideration of wind hazard-induced financial loss on the part of governments, the construction industry, and the insurance industry, who could use its analyzed results and applied methodology to mitigate financial losses from unexpected extreme events. Specifically, insurance companies can use the developed vulnerability model to inform their risk weight models of chosen areas, allocating wind hazard-prone areas, setting appropriate premiums, and estimating potential losses to insured properties. Construction companies can assess possible wind-storm risks to their construction costs and schedules; and governments can refer to the simplified quantitative vulnerability curves developed in the present study to optimize their disaster planning on a national scale.

Nevertheless, some limitations of this research should be acknowledged. First, it focused on the impact of a single typhoon on a single metropolitan area, and its approach therefore may not be able to accurately account for damage from other typhoons, from other types of storms, or in other parts of the world. Therefore, more case studies are needed – as are curves that incorporate construction-typology and building-use data (i.e., residential, commercial or industrial) into their damage ratios. If each building-use category has its own damage ratio, that ratio can have its own curves tailored to the vulnerability of each of the construction types prevailing in that category; and comparing vulnerability models across similar construction types may yield important insights. However, a thorough analysis

of construction typology would require larger amounts of data than are typically available to researchers. Future research should also consider various additional aspects of wind profiles, including wind direction, as independent variables in the estimation of wind-induced damage. The historical paths of severe typhoons, and/or synthetic typhoons' tracks, could also be important indicators typhoons' and other wind hazards' intensities. Due consideration of such additional damage indicators could well improve the overall accuracy of models of this kind. Also, a combination of analytical, empirical, and hybrid approaches could mitigate the drawbacks of using any one of them by itself. Lastly, the proposed approach could be usefully combined with tidal-gauge data to estimate the return periods of the damaging storm surges often associated with extreme wind storms, as doing so would further increase the accuracy of natural disaster-related damage estimation, and even potentially help prevent property damage and loss of life.

References

[1] Blake, E. S., Rappaport, E. N., Landsea, C. W., and NHC Miami. 2007. The deadliest, costliest, and most intense United States tropical cyclones from 1851 to 2006 (and other frequently requested hurricane facts). NOAA Technical Memorandum NWS TPC-5. Miami, FL: National Weather Service, National Hurricane Center.

[2] Kim, J. M., Kim, T., and Son, K. 2017. "Revealing building vulnerability to windstorms through an insurance claim payout prediction model: A case study in South Korea." *Journal of Geomatics*, Natural Hazards and Risk. 8 (2), 1333–1341. https://doi.org/10.1080/19475705.2017.1337651.

[3] Cummins, J. D., Lewis, C. M., and Phillips, R. D. 1999. "Pricing excess-of-loss reinsurance contracts against catastrophic loss." In The Financing of Catastrophe Risk edited by Froot, K. A. 93-148. Cambridge, MA: University of Chicago Press.

[4] Kim, J. M., Woods, P. K., Park, Y. J., and Son, K. Y. 2016. "Estimating the Texas Windstorm Insurance Association (TWIA) claim payout of commercial buildings from Hurricane Ike." *Natural Hazards*. 84, 405–424. https://doi.org/10.1007/s11069-016-2425-7.

[5] Khanduri, A.C., and Morrow, G.C. 2003. "Vulnerability of buildings to windstorms and insurance loss estimation." *Journal of Wind Engineering and Industrial Aerodynamics*. 91 (4), 455–467. https://doi.org/10.1016/S0167-6105(02)00408-7.

[6] Lopeman, M., and Deodatis, G. 2015. "Extreme storm surge hazard estimation and windstorm vulnerability assessment for quantitative risk analysis." Doctoral Dissertation. Columbia University, New York, NY.

[7] Jaimes, M. A., García-Soto, A. D., and Osvaldo Martín del Campo, J. 2019. "Probabilistic risk assessment on wind turbine towers subjected to cyclone-induced wind loads." *Wind Energy*. 23, 528-546. DOI: 10.1002/we.2436.

[8] Goyal, P., and Datta, T. K. 2013. "Effect of Wind Directionality on the Vulnerability of Rural Housed due to Cyclonic Wind." *Natural Hazards Review.* 14 (4). 258-267. DOI: 10.1061/(ASCE)NH.1527-6996.0000103.

[9] Kim, J.-M., Kim, T., Son, K., Yum, S.-G, and Ahn, S. 2019. "Measuring Vulnerability of Typhoon in Residential Facilities: Focusing on Typhoon Maemi in South Korea." *Sustainability*. 11, 2768. doi:10.3390/su11102768

[10] Ahn, S., Kim, T., and Kim, J.-M. 2020. “Sustainable Risk Assessment through the Analysis of Financial Losses from Third-Party Damage in Bridge Construction.” *Sustainability*. 12, 2435. doi:10.3390/su12083435

[11] Friedman, D. G. 1975. “Computer simulation of natural hazard assessment” Institute of Behavioral Science, University of Colorado, Boulder, CO. 192-194.

[12] Leicester, R.L., and Reardon, G.F. 1976. “A statistical analysis of the structural damage by Cyclone Tracy.” Proceedings, Annual Civil Engineering Conference Institution of Engineers Australia, Barton, 18(2), 50–54.

[13] Hart, G.C. 1976. “Estimation of structural damage due to tornadoes”. Proceedings, Symposium on Tornadoes: Assessment of Knowledge and Implications for Man, Texas Tech University, TX, 645–665.

[14] Sparks, P. R., Schiff, S. D., and Reinhold, T. A. 1994. “Wind damage to envelopes of houses and consequent insurance losses.” *Journal of Wind Engineering & Industrial Aerodynamics.* 53, 145–155.

[15] Vickery, P.J., Lin, J., Skerlj, P.F., Twisdale, L.A., and Huang, K. 2006a. “HAZUS-MH hurricane model methodology. I: Hurricane hazard, terrain, and wind modelling.” *Natural Hazards Review*. 7 (2), 82–93. doi:10.1061/(ASCE)1527 6988(2006)7:2(82).

[16] Vickery, P. J., Skerlj, P. F., Lin, J., Twisdale Jr., L. A., Young, M. A., and Lavelle, F. M. 2006b. “HAZUS-MH hurricane model methodology. II: Damage and loss estimation.” *Natural Hazards Review*. 7 (2), 94–103. https://doi.org/10.1061/(ASCE)1527-6988(2006)7:2(94).

[17] Henderson, D., and Ginger, J. 2007. “Vulnerability model of an Australian high-set house subjected to cyclonic loading.” *Wind and Structures An international Journal*. 10 (3), 269-285. doi:10.12989/was.2007.10.3.269

[18] Heneka, P., and Ruck, B. 2008. “A damage model for the assessment of storm damage to buildings.” *Engineering Structures.* 30 (12), 3603-3609. https://doi.org/10.1016/j.engstruct.2008.06.005

[19] Walker, G. R. 2011. “Modelling the vulnerability of buildings to wind – a review”. *Canadian Journal of Civil Engineering*. 38, 1031–1039.

[20] Watson, C. C., and Johnson, M. E. 2004. “Hurricane loss estimation models: Opportunities for improving the state of the art.” *Journal of Bulletin of the American Meteorological Society*. 85 (11), 1713–1726. https://doi.org/10.1175/BAMS-85-11-1713.

[21] Hwang, Y., and Deodatis, G. 2013. “Stochastic analysis of storm-surge induced infrastructure losses in New York City.” Doctoral Dissertation. Columbia University, New York, NY.

[22] Rhee, D. M., and Lombardo, F. T. 2018. “Improved near-surface wind speed characterization using damage patterns.” *Journal of Wind Engineering & Industrial Aerodynamics*. 180, 288-297. https://doi.org/10.1016/j.jweia.2018.07.017.

[23] Cui, W., and Caracoglia, L. 2016. “Exploring hurricane wind speed along US Atlantic coast in warming climate and effects on predictions of structural damage and intervention costs.” *Engineering Structures.* 122, 209-225. http://dx.doi.org/10.1016/j.engstruct.2016.05.003.

[24] Dunn, S., Wilkinson, S., Alderson, D., Fowler, H., and Galasso, C. 2018. “Fragility Curves for Assessing the Resilience of Electricity Networks Constructed from an Extensive Fault Database.” *Natural Hazards Review.* 19 (1). 04017019. DOI: 10.1061/(ASCE)NH.1527-6996.0000267.

[25] Cai, Y., Xie, Q., Xue, S., Hu, L., and Kareem, A. 2019. “Fragility modelling framework for transmission line towers under winds.” *Engineering Structures*. 191, 686-697. https://doi.org/10.1016/j.engstruct.2019.04.096.

[26] Suvanto, S., Peltoniemi, M., Tuominen, S., Strandström, M., and Lehtonen, A. 2019. “High-resolution mapping of forest vulnerability to wind for disturbance aware forestry.” *Forest Ecology and Management.* 453, 117619. https://doi.org/10.1016/j.foreco.2019.117619.

[27] Khajwal, A. B., and Noshadravan, A. 2020. “Probabilistic Hurricane Wind-Induced Loss Model for Risk Assessment on a Regional Scale.” *Journal of Risk and Uncertainty in Engineering Systems.* 6(2), 04020020. DOI: 10.1061/AJRUA6.0001062.

[28] Mitsova, D., Esnard, A,-M., Sapat, A., and Lai, B. S. 2018. “Socieconomic vulnerability and electric power restoration timelines in Florida: the case of Hurricane Irma.” *Natural Hazards.* 94, 689-709. https://doi.org/10.1007/s11069-018-3413-x(0123456789().,-volV)(0123456789().,-volV).

[29] Hatzikyriakou, A., and Lin, N. 2019. ″Multi-hazard analysis of tropical cyclone return periods.” Proceedings, International Association for Bridge and Structural Engineering, IABSE Congress. New York.

[30] Ku, H., Lee, S., and Lee, Y. K. 2008. “Statistical model and characteristics of typhoon-induced rainfall around the Korean peninsula.” *Korean Journal of Society of Hazard Mitigation*. 8 (5), 45–51.

[31] Park, J. G., Jeong, W. S., Kim, E. B., and Kim, J. S. 2011. “A study on possible regional disaster prediction for the accompanying high winds in the storm.” *Asia-Pacific Journal of Atmospheric Sciences.* 10 (1), 306–307.

[32] Park, J. G., Jeong, W. S., Kim, J. S., and Kim, E. B. 2012. “The trend of damage cost during Typhoon period affected in the Korean Peninsula.” *Asian Journal of Atmospheric Environment*. 5, 152.

[33] Shin, H., Lee, W., Byun, G., Kim, J., Jang, K., and Lee, J. 2013. “Evaluation of the numerical models’ typhoon track predictability based on the moving speed and direction.” *Asia-Pacific Journal of Atmospheric Sciences.* 10, 372–373.

[34] Kim, J. M., Woods, P. K., Park, Y. J., Kim, T., and Son, K. 2015. “Predicting hurricane wind damage by claim payout based on Hurricane Ike in Texas.” *Geomatics, Natural Hazards and Risk*. 7 (5), 1513–1525. https://doi.org/10.1080/19475705.2015.1084540.

[35] Kim, J. M., Son, K. Y., and Kim, Y. J. 2018. “Assessing regional typhoon risk of disaster management by clustering typhoon paths.” *Journal of Environment, Development and Sustainability*. 21 (5), 2083–2096. https://doi.org/10.1007/s10668-018-0086-2.

[36] Burton, C. G. 2010. “Social vulnerability and hurricane impact modeling.” *Natural Hazards Review.* 11 (2), 58–68. https://doi.org/10.1061/(ASCE)1527-6988(2010)11:2(58).

[37] Dunion, J. P., Landsea, C. W., Houston, S. H., and Powell, M. D. 2003. “A reanalysis of the surface winds for Hurricane Donna of 1960.” *Monthly Weather Review*. 131 (9). https://doi.org/10.1175/1520-0493(2003)131<1992:AROTSW>2.0.CO;2.

[38] Rego, J. L., and Li, C. 2009. “On the importance of the forward speed of hurricanes in storm surge forecasting: A numerical study.” *Geophysical Research Letters*. 36 (7), L07609. https://doi.org/10.1029/2008GL036953.

[39] Choi, O., and Fisher, A. 2003. “The impacts of socioeconomic development and climate change on severe weather catastrophe losses: Mid-Atlantic Region (MAR) and the US.” *Journal of Climatic Change*. 58 (1), 149–170. https://doi.org/10.1023/A:1023459216609.

[40] Huang, Z., Rosowsky, D. V., and Sparks, P.R. 2001. “Hurricane simulation techniques for the evaluation of wind-speeds and expected insurance losses.” *Journal of Wind Engineering and Industrial Aerodynamic*. 89 (7), 605–617. https://doi.org/10.1016/S0167-6105(01)00061-7.

[41] Powell, M. D., and Houston, S. H. 1998. “Surface wind fields of 1995 hurricanes Erin, Opal, Luis, Marilyn, and Roxanne at landfall.” *Monthly Weather Review*. 126 (5), 1259–1273. https://doi.org/10.1175/1520-0493(1998)126<1259:SWFOHE>2.0.CO;2.

[42] Powell, M. D., Houston, S. H., Amat, L. R., and Morisseau-Leroy, N. 1998. “The HRD real-time hurricane wind analysis system.” *Journal of Wind Engineering and Industrial Aerodynamics*. 77 and 78, 53–64. https://doi.org/10.1016/S0167-6105(98)00131-7.

[43] Powell, M. D., Murillo, S., Dodge, P., Uhlhorn, E., Gamache, J., Cardone, V., Cox, A., Otero, S., Carrasco, N., Annace, B., and St. Fleur, R. 2010. “Reconstruction of Hurricane Katrina’s wind fields for storm surge and wave hindcasting.” *Journal of Ocean Engineering*. 37 (1), 26–36. https://doi.org/10.1016/j.oceaneng.2009.08.014.

[44] De Silva, D. G., Kruse, J. B., and Wang, Y. 2008. “Spatial dependencies in wind-related housing damage.” *Natural Hazards*. 47 (3), 317–330. https://doi.org/10.1007/s11069-008-9221-y.

[45] Ayalew, L., and Yamagishi, H. 2005. “The application of GIS-based logistic regression for landslide susceptibility mapping in the Kakuda-Yahiko Mountains, Central Japan.” *Journal of Geomorphology*. 65 (1), 15–31. https://doi.org/10.1016/j.geomorph.2004.06.010.

[46] Cui, B., Wang, C., Tao, W., and You, Z. 2009. “River channel network design for drought and flood control: A case study of Xiaoqinghe River basin, Jinan City, China.” *Journal of Environmental Management*. 90 (11), 3675–3686. https://doi.org/10.1016/j.jenvman.2009.07.010.

[47] Dai, F.C., Lee, C.F., and Ngai, Y.Y. 2002. “Landslide risk assessment and management: An overview.” *Journal of Engineering Geology*. 64 (1), 65–87. https://doi.org/10.1016/S0013-7952(01)00093-X.

[48] Zhai, G., Fukuzono, T., and Ikeda, S. 2007. “Multi-attribute evaluation of flood management in Japan: A choice experiment approach.” *Water and Environment Journal*. 21 (4), 265–274. https://doi.org/10.1111/j.1747"-6593.2007.00072.x.

[49] Keim, B. D., Muller R. A., and Stone, G. W. 2007. “Spatiotemporal patterns and return periods of tropical storm and hurricane strikes from Texas to Maine.” *Journal of Climate*. 20 (14), 3498–3509. https://doi.org/10.1175/JCLI4187.1.

[50] Noel, J. M., Maxwell, A., Platt, W. J., and Pace, L. 1994. “Effects of Hurricane Andrew on cypress (taxodium distichum var. nutans) in south Florida.” *Journal of Coast Research*. 21, 184–196.

[51] D’Ayala D., Copping A., and Wang H. 2006. “A conceptual model for multi-hazard assessment of the vulnerability of historic buildings.” Proceedings, the Structural Analysis of Historical Constructions: Possibilities of Numerical and Experimental Techniques, the Fifth International Conference. New Delhi, 121–140.

[52] Vamvatsikos, D., and Fragiadakis, M. 2010. “Incremental dynamic analysis for estimating seismic performance sensitivity and uncertainty.” *Earthquake Engineering and Structural Dynamics*. 39, 141–163.

[53] Dolšek, M. 2012. “Simplified method for seismic risk assessment of buildings with consideration of aleatory and epistemic uncertainty.” *Structure and Infrastructure Engineering*. 8 (10), 939-953. DOI: 10.1080/15732479.2011.574813

[54] Klir, G. J. 2006. “Uncertainty and Information.” John Wiley & Sons, Hoboken, New Jersey.

[55] Basoz, N., and Kiremidjian, A. S. 1997. “Risk assessment of bridges and highway systems from the Northridge earthquake.” Proceedings, 2nd National Seismic Conference on Bridges and Highways, Transportation Research Board, Washington, DC.

[56] Shinozuka, M. Feng, M. Q., and Lee J., and Naganuma, T. 2000. “Statistical Analysis of Fragility Curves.” *Journal of Engineering Mechanics*. 126 (12), 1224–1231. https://doi.org/10.1061/(ASCE)0733-9399(2000)126:12(1224).

[57] Porter, K., Kennedy, R., and Bachman, R. 2007. “Creating fragility functions for performance-based earthquake engineering.” *Earthquake Spectra*. 23(2), 471–489.

[58] Lin, J. H. 2008. “Seismic fragility analysis of frame structures.” *International Journal of Structural Stability and Dynamics*. 8(3), 451–463.

[59] Ellingwood, B., Rosowsky, D., Li, Y., and Kim, J. 2004. “Fragility assessment of light-frame wood construction subjected to wind and earthquake hazards.” *Journal of Structural Engineering*. 130(12), 1921–1930.

[60] Holmes, J. 1996. “Vulnerability curves for buildings in tropical cyclone regions.” Probabilistic Mechanics and Structural Reliability: Proceedings, 7th ASCE EMD/STD Specialty Conference, Worcester, MA, 78–81.

[61] Pinelli, J.-P., Simiu, E., Gurley, K., Subramanian, C. 2004. “Hurricane damage prediction model for residential structures.” *Journal of Structural Engineering*. 130(11), 1685–1691.

[62] Li, Y., and Ellingwood, B. R. 2006. “Hurricane damage to residential construction in the US: Importance of uncertainty modeling in risk assessment.” *Engineering Structures*. 28(7), 1009–1018.

[63] Katz, R. W. 2002. “Stochastic modeling of hurricane damage.” *Journal of Applied Meteorology*. 41 (7), 754–762. https://doi.org/10.1175/1520-0450(2002)041<0754:SMOHD>2.0.CO;2.

[64] Wang, C., H. Zhang, K. Feng, and Q. Li. 2017. “Assessing hurricane damage costs in the presence of vulnerability model uncertainty.” Natural Hazards. 85 (3), 1621–1635. https://doi.org/10.1007/s11069-016-2651-z.

[65] Grossi, P., and Kunreuther, H. 2005. “Catastrophe modeling: A new approach to managing risk.” Springer, New York.

[66] Nishijima, K., Maruyama, T., Graf, M., 2012. “A preliminary impact assessment of typhoon wind risk of residential buildings in Japan under future climate change.” *Hydrological Research Letters*. 6, 23–28.